ISSN 1674-1056
http://cpb.iphy.ac.cn
http://iopscience.iop.org/cpb
中国物理 B
Chinese Physics
中国物理 Chinese Physics B

Coherent control of fragmentation of methyl iodide by shaped femtosecond pulse train

Qiu-Nan Tong(佟秋男), De-Hou Fei(费德厚), Zhen-Zhong Lian(廉振中), Hong-Xia Qi(齐洪霞), Sheng-Peng Zhou(周胜鹏), Si-Zuo Luo(罗嗣佐), Zhou Chen(陈洲), Zhan Hu(胡湛)

Citation: Chin. Phys. B . 2019, 28(9): 093201 . **doi:** 10.1088/1674-1056/28/9/093201
Journal homepage: http://cpb.iphy.ac.cn; http://iopscience.iop.org/cpb

What follows is a list of articles you may be interested in

Controlling Rydberg excitation process with shaped intense ultrashort laser pulses

Xiao-Yun Zhao(赵晓云), Chun-Cheng Wang(王春成), Shi-Lin Hu(胡师林), Wei-Dong Li(李卫东), Jing Chen(陈京), Xiao-Lei Hao(郝小雷)

Chin. Phys. B . 2019, 28(8): 083202 . **doi:** 10.1088/1674-1056/28/8/083202

Dependence of photoelectron-momentum distribution of H_2^+ molecule on orientation angle and laser ellipticity

Hong-Dan Zhang(张宏丹), Si-Qi Zhang(张思琪), Lei Ji(纪磊), Qi Zhen(甄琪), Jing Guo(郭静), Xue-Shen Liu(刘学深)

Chin. Phys. B . 2019, 28(5): 053201 . **doi:** 10.1088/1674-1056/28/5/053201

Femtosecond strong-field coherent control of nonresonant ionization with shaped pulses

Qiu-Nan Tong(佟秋男), Zhen-Zhong Lian(廉振中), Liang Zhao(赵亮), Hong-Xia Qi(齐洪霞), Zhou Chen(陈洲), Zhan Hu(胡湛)

Chin. Phys. B . 2019, 28(3): 033201 . **doi:** 10.1088/1674-1056/28/3/033201

Angle-resolved spectra of the direct above-threshold ionization of diatomic molecule in IR+XUV laser fields

Shang Shi(石尚), Fa-Cheng Jin(金发成), Bing-Bing Wang(王兵兵)

Chin. Phys. B . 2019, 28(2): 023202 . **doi:** 10.1088/1674-1056/28/2/023202

Validity of extracting photoionization time delay from the first moment of streaking spectrogram

Chang-Li Wei(魏长立), Xi Zhao(赵曦)

Chin. Phys. B . 2019, 28(1): 013201 . **doi:** 10.1088/1674-1056/28/1/013201

Coherent control of fragmentation of methyl iodide by shaped femtosecond pulse train*

Qiu-Nan Tong(佟秋男)[1,2], De-Hou Fei(费德厚)[1,2], Zhen-Zhong Lian(廉振中)[1,2], Hong-Xia Qi(齐洪霞)[1,2], Sheng-Peng Zhou(周胜鹏)[1], Si-Zuo Luo(罗嗣佐)[1], Zhou Chen(陈洲)[1,2,†], and Zhan Hu(胡湛)[1,2,‡]

[1] *Institute of Atomic and Molecular Physics, Jilin University, Changchun* 130012, *China*

[2] *Advanced Light Field and Modern Medical Treatment Science and Technology Innovation Center of Jilin Province, Jilin University, Changchun* 130012, *China*

(Received 30 April 2019; revised manuscript received 25 June 2019; published online 20 August 2019)

Coherent control of fragmentation of CH_3I using shaped femtosecond pulse train is investigated. The dissociation processes can be modulated by changing the separation of the shaped pulse train, and the yield of I^+ under the irradiation of the optimal pulse is significantly increased compared with that using the transform-limited pulse. We discuss the control mechanism of dissociation processes with coherent interference in time domain. A three-pulse control model is proposed to explain the counterintuitive experimental results.

Keywords: coherent control, fragmentation, shaped pulse

PACS: 32.80.Rm, 42.50.Hz **DOI:** 10.1088/1674-1056/ab33f3

1. Introduction

The control of molecular fragmentation induced by laser is a fundamental goal with many important applications in controlling physical, chemical, and biological processes. The selective breaking and reforming of chemical bonds are the key of molecular fragmentation control, which can be used to exclusively acquire the desired products. However, due to the complexity of the molecular structure, it is quite difficult to control the dissociation processes using a single simple infrared laser pulse. The combination of developed detection techniques and state-of-the art laser manipulation techniques makes the control possible. Many different detection methods have been employed to probe the photodissociation processes, such as time-of-flight mass spectroscopy (TOFMS) with high resolution of species,[1] ion velocity map imaging (VMI),[2,3] and photoelectron photoion coincidence (PEPICO).[4–6] On the other hand, a large variety of laser fields have been used to study the photodissociation dynamics. For instance, the linearly or circularly polarized chirped laser pulses enhanced the dissociation by ladder climbing.[7] A weak ultraviolet (UV) laser combined with an intense infrared (IR) laser could facilitate the dissociation processes.[8] There are also many research works on dissociation processes using extreme ultraviolet laser (XUV),[9–11] single-cycle terahertz laser, and few-cycle laser with controllable carrier envelope phase (CEP).[12,13]

Coherent control is a robust method of controlling dissociation processes using multiple quantum pathways interference, which can enhance the desired process among the different competition processes. In the past, bond-selected chemistry has been extensively studied by both experiment[14,15] and theory.[16,17] For example, the branching ratios of dissociation processes can be manipulated by the dynamic Stark effect,[18] conical intersections induced by laser,[19] and coherent adiabatic passage.[20] The development in laser pulse shaping techniques promotes the coherent control of chemical reactions. By the pulse shaping techniques, one can stretch the pulse from tens of femtoseconds to tens of picoseconds, and modulate the linear chirp and the relative phase of the laser pulses. Therefore, we can design the laser pulses to achieve arbitrary chemical bond breaking by selectively introducing energy into the molecule system. The optimal control theory (OCT)[21] has emerged to achieve the selective control without the prediction of the fragmentation mechanism. The closed-loop optimal feedback control steers the dissociation towards a pre-designed product. So far, there have been many closed-loop control experiments and theories for different molecules.[22] Due to the breakthrough of the few-cycle carrier envelope phase (CEP) stable laser, one can modulate the dissociation processes by controlling the CEP of the ultrafast optical field. For instance, Xie and co-workers[23] found that the variation of CEP can selectively remove the rescattering energy of special valence electrons and achieve the control of molecular fragmentation processes.

Methyl iodide (CH_3I), as a polar molecule with C_{3v} symmetry, has been extensively studied. The dissociation processes were investigated via high-resolution TOFMS,[1] ion VMI,[2] and zero kinetic energy (ZEKE) spectra,[24] which enables us to acquire the knowledge of the molecular poten-

*Project supported by the National Natural Science Foundation of China (Grant No. 11374124).

†Corresponding author. E-mail: phy_cz@jlu.edu.cn

‡Corresponding author. E-mail: huzhan@jlu.edu.cn

© 2019 Chinese Physical Society and IOP Publishing Ltd

tial energy curves and dissociation mechanism. The A-band photodissociation is a typical topic for studying the dissociation dynamics of CH_3I.[25–27] The A-band photodissociation results in two different dissociation pathways: (i) the strong parallel transition to the $^3Q_0$ state that produces CH_3 and spin–orbit excited $I^*(^2P_{1/2})$; (ii) the weak perpendicular transitions to the $^3Q_1$ and $^1Q_1$ states that produce CH_3 and ground state $I(^2P_{3/2})$. The control of the two dissociation pathways has been carried out with nanosecond lasers and two femtosecond lasers using the pump–probe technique. When the pulses are shorter than 100 fs, compared to direct photodissociation, the molecule is more likely to first ionize to yield the molecular ion and then subsequently dissociate into fragment ions. The dissociation dynamics of molecular ion CH_3I^+ induced by intense few-cycle laser have been studied,[28] which demonstrates that the spin–orbit states of C–I dissociation can be selectively modulated. The dissociative ionization (DI) and Coulomb explosion (CE) of CH_3I have been investigated using VMI and femtosecond XUV spectroscopy.[10] Some theoretical work of the potential energy surfaces has also been reported.[9]

The aim of this work is to investigate the dissociation dynamics of CH_3I irradiated by shaped femtosecond pulse trains. By analyzing the kinetic energy releases (KER) of the fragment ion I^+, we can identify the DI and CE channels using the transform-limited (TL) and shaped femtosecond pulse train. Moreover, the dissociation process can be modulated by changing the sub-pulse separation, and the yield of I^+ irradiated by the optimal pulse is significantly increased compared with that using TL pulse. The modulation mechanism of the dissociation process is discussed based on coherent interference in time domain. A three-pulse control model is proposed to explain the counterintuitive experimental results.

2. Experimental setup

The experimental setup, depicted schematically in Fig. 1, has been described in detail elsewhere.[29] Briefly, our experiments are performed using a standard VMI system similar to that of Eppink.[2] The mixture of 10% CH_3I seeded in He, at a stagnation pressure of 4 bar, is expanded into the source chamber through a pulsed valve (General Valve Series 9, 0.5 mm orifice). Before entering the interaction chamber, the supersonic molecular beam is directed through a 0.5 mm skimmer. The ions generated in the interaction region are extracted and accelerated using the electrostatic lens system at the end of the TOF tube and projected onto a 2D detector composed of two microchannel plates (MCPs) in a chevron configuration coupled to a phosphor screen. The mass spectrometry is obtained and averaged by connecting the photomultiplier tube (PMT), which transfers to the oscilloscope output with the computer.

The laser system is a Ti: sapphire chirped-pulse amplification laser (Millennia feed laser, Spectra-Physics Tsunami oscillator, and Spitfire amplifier) with the central wavelength of 800 nm, the pulse duration of 100 fs, and the repetition rate of 1 kHz. The laser pulse from the oscillator is directed into the pulse shaper and the shaped pulse is generated. Then, the shaped pulse passes through the amplifier, after which the energy of the single pulse can reach 200 μJ. Finally, the laser beam is focused via a lens with a focal length of 25 cm into the interaction chamber. The pulse shaper in the present experiments is similar to that used in our previous work. The pulse is shaped by a dual-mask spatial light modulator (CRI Inc., SLM-640). A pair of cylindrical lenses ($f = 300$ mm) and gratings (2000 grooves/mm) are used to spectrally disperse (at the input) and recollimate (at the output) the laser pulse. A train of three equally spaced femtosecond laser pulses is used to control the CH_3I molecular dissociation in our experiment. The multiphoton intrapulse interference phase scan (MIIPS) method[30,31] is used to ensure that a pulse without any phase through the pulse shaper is still a TL pulse.

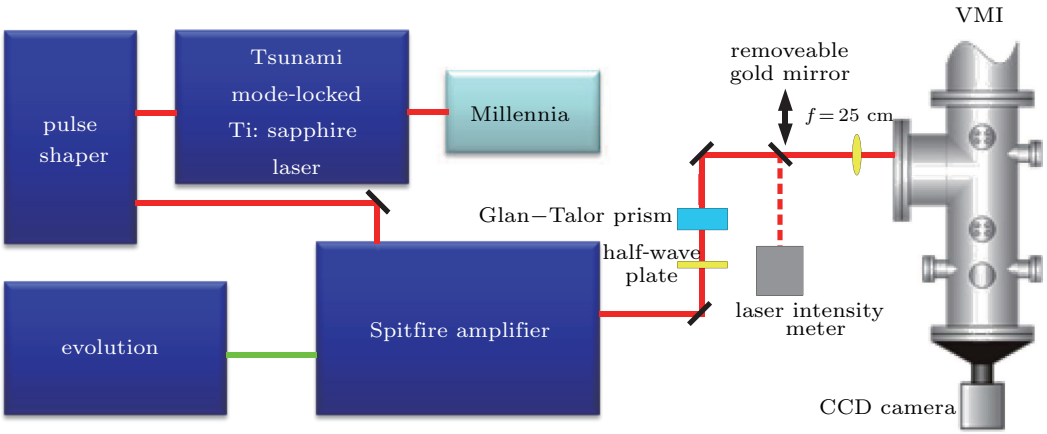


Fig. 1. Schematic diagram of the experimental setup. The pulse shaper is placed between oscillator and amplifier. The shaped pulse is focused into the VMI setup. A half-wave plate and a Glan–Talor prism are used to change the laser intensity. A removeable gold mirror is used to reflect the laser pulse into the laser intensity meter for energy measurement.

3. Results and discussion

3.1. Fragmentation with a TL pulse

In this section, a detailed analysis of TL laser-induced fragmentation of CH_3I is presented. The intensity of the TL pulse at the focal point is about 7×10^{13} W·cm^{-2}, which is our intentional decision based on the experimental research. Our aim is to study the modulation of fragmentation induced by two mechanisms using shaping pulse when the DI (strong) and the CE (weak) processes are simultaneously present. The 2D velocity images of fragment ion I^+ are measured using the VMI system. By analyzing the KER distribution of the fragment ion, we can identify the dissociation channels. The KER distribution extracted from the 2D velocity images by the integration over the full range of angle is shown in Fig. 2, which carries two distinctive peaks, one at low kinetic energy and the other at high kinetic energy. The peak at low kinetic energy exhibits a more obvious shoulder than that at high kinetic energy. Liu and co-works[32] proposed that each dissociation channel corresponds to a Gaussian peak in the KERS distribution. In the present experiment, a Gaussian distribution is assumed for each channel

$$G_q(p,q) = \frac{2C}{W\sqrt{2}} \exp\left[-\frac{(E-E_0)^2}{W^2}\right], \tag{1}$$

where $G_q(p,q)$ denotes the charge numbers of the CH_3^{p+} and I^{q+} fragments from the dissociation channel, E_0 and W are the peak value and the FWHM of the KER distribution, respectively, and C is the normalization factor. As shown in Fig. 2, the combination of four Gaussian distributions of Eq. (1) achieves a almost perfect fit for the four I^+ KER distribution.

In the following section, each individual channel producing fragment ion I^+ is identified. When the intensity of the TL pulse is weak, the dissociation processes of CH_3I follow the multiphoton DI mechanism. Therefore, the CH_3I molecule is first ionized to produce the parent ion CH_3I^+, and then dissociated via additional photon absorption. But when the intensity of the TL pulse is strong, the parent ion is continuously ionized to form a higher charged parent ion and then produce the I^+ fragment with higher kinetic energy by CE. We define the fragmentation channel of I^+ as $G_q(p,q)$: $CH_3I^{(p+q)+} \rightarrow CH_3^{p+}+I^{q+}$.

The values of two peaks in the low kinetic energy region from Fig. 2 are 0.08 eV and 0.21 eV, which belong to the two DI channels $G_1(0,1)$ and $G_1(0,1')$. Because the intensities of the two peaks hardly change with the increase of the laser intensity, those of the CE channels will increase. The intermediate ionized $CH_3I^+(X)$ ion of the DI channel resides temporally in the vibrational ground state which consists of the spin orbit rotational manifold (lower $^2E_{3/2}$ and upper $^2E_{1/2}$). Since the rotational constants of $CH_3I^+(X)$, $A = 5.200$ cm^{-1} and $B = 0.253$ cm^{-1}, are almost the same as those of $CH_3I(X)$, $A = 5.174$ cm^{-1} and $B = 0.250$ cm^{-1}, the probability of the vertical transition is larger due to the higher Franck–Condon factor. Table 1 shows the theoretical dissociation energies and KER distributions of DI channels resulting from the three (or two) photons excitations of $CH_3I^+(X, ^2E_{3/2})$ and $CH_3I^+(X, ^2E_{1/2})$ parent ions, as well as the experimental KER distributions of our work and other research groups for comparison. Therefore, the two DI channels $G_1(0,1)$ and $G_1(0,1')$ correspond to $CH_3I^+(X, ^2E_{3/2}) \rightarrow CH_3(^2A'')+I^+(^3P_{1,0})$ and $CH_3I^+(X, ^2E_{3/2}) \rightarrow CH_3(^2A'')+I^+(^3P_2)$, respectively.

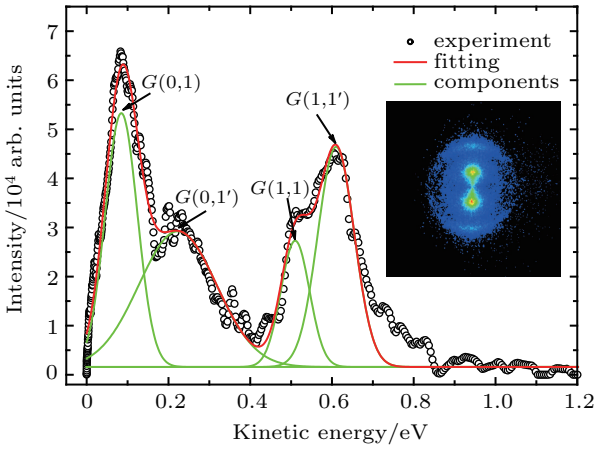


Fig. 2. The KER distribution extracted from the 2D velocity image using TL pulse. Black circle is the experimental curve, and the red solid line is the fit curve. The green solid lines indicate the four components of Gaussian distributions with Eq. (1). The inset is the ion velocity image using TL pulse.

Table 1. The calculated I^+ KERs of the n-photon dissociation channels of CH_3I^+ and the observed I^+ KERs by Liu *et al.*,[31] Wang *et al.*,[32] and in the present work.

Dissociation channels of CH_3I^+	Dissociation energy/eV	n	Calculated KER/eV	Experimental KER/eV		
				Liu	Wang	Our work
$CH_3I^+(X, ^2E_{1/2}) \rightarrow CH_3(^2A'')+I^+(^3P_2)$	0.39	2	0.04		0.03	
$CH_3I^+(X, ^2E_{3/2}) \rightarrow CH_3(^2A'')+I^+(^3P_2)$	1.32	3	0.14		0.16	0.21
$CH_3I^+(X, ^2E_{1/2}) \rightarrow CH_3(^2A'')+I^+(^3P_{1,0})$	1.11	3	0.11		0.09	
$CH_3I^+(X, ^2E_{3/2}) \rightarrow CH_3(^2A'')+I^+(^3P_{1,0})$	0.48	3	0.07	0.07± 0.03		0.08

The values of two peaks in the high kinetic energy region from Fig. 2 are 0.51 eV and 0.61 eV, which belong to the two channels $G_1(1,1)$ and $G_1(1,1')$ resulting from the CE of CH_3I^{2+}. Table 2 shows the experimental KER distributions of the CE channels, where the KER distributions obtained from other research groups are smaller than that obtained in our

work. The laser pulse duration is 180 fs in the experiment of Liu group, 35 fs and 50 fs in the experiments of Wang *et al.* and Corrales *et al.*, which indicates that the differences in the KER distributions are not due to the laser pulse duration. Comparing the KER distributions with those in our experiment in Fig. 2, one can find that the right side of the fit curve is absent. We propose that it can be attributed to the contribution of higher charged CE channels.

Table 2. The I^+ KERs of CE channels observed by Liu *et al.*,[32] Wang *et al.*,[33] Corrales *et al.*,[19] and in the present work.

Coulomb explosion channels (p,q)	Experimental KER/eV			
	Our work	Liu *et al.*	Wang *et al.*	Corrales *et al.*
$CH_3I^{2+} \rightarrow CH_3^+ + I^+(^3P_{1,0}),\ G(1,1)$	0.51			0.46
$CH_3I^{2+} \rightarrow CH_3^+ + I^+(^3P_2),\ G(1,1')$	0.61	0.43	0.46	0.55

3.2. Coherent control of fragmentation with shape pulse train

A pulse train with evenly spaced sub-pulses is produced experimentally with the sinusoidal phase function[34]

$$\varphi(\omega) = A\sin[(\omega - \omega_{\text{ref}})T + \phi], \tag{2}$$

where A defines the amplitude of the modulation function, T is the frequency of the sinusoidal function oscillation, and φ is the constant phase offset. The ω_{ref} is introduced experimentally to describe the initial reference angular frequency of the sinusoidal phase function with respect to the central angular frequency of the laser spectrum. The temporal separation between sub-pulses is determined by the parameter T. In order to select a pulse train that can be used to control the fragmentation, we fix A at 1.2566, which generates a three-pulse train. The envelope of each sub-pulse is a replica of the unmodulated pulse envelope with reduced intensity, and the difference of relative phases between adjacent sub-pulses is determined by $\Delta\omega T + \phi$, where $\Delta\omega = \omega_0 - \omega_{\text{ref}}$ denotes the difference between the laser carrier frequency and the reference frequency of the sinusoidal phase function. The φ is fixed at 0, then the difference of relative phases is determined by $\Phi_{\text{dif}} = \Delta\omega T$.

In this section, we present the experimental KER distributions obtained under the shaped pulse train with the same energy as that of the TL pulse. By scanning the value of T from about 150 fs to 440 fs, the KER distributions upon the variation of the pulse separation are mapped in Fig. 3. When the pulse separation is small ($<$ 190 fs) or large ($>$ 300 fs), the intensities of I^+ are so weak that the peaks are absent. For the pulse separation ranging from 190 fs to 300 fs, the KER distributions are similar to those under the TL pulse, and all distributions show two main peaks corresponding to the DI channels (low energy peak) and CE channels (high energy peak), respectively. The peak positions hardly change with the variation of the pulse separation with respect to those under the TL pulse. Moreover, there is an optimal pulse train (at $T = 208$ fs) that makes the two peaks simultaneously reach the maxima, which indicates that the shaped pulse train can achieve the modulation of the KER distribution of the I^+ fragment. We also find that the intensity of CE channel's peak is generally stronger than that of DI channel's peak for the shaped pulse train, which is exactly the opposite to the case for the TL pulse (shown in Fig. 2). Figure 4 shows the KER distributions using the TL pulse and optimal pulse train, where the intensities of the vertical axis represent the counts of VMI. Counterintuitively, both intensities of the DI and CE channels using the shaped pulse train are nearly an order of magnitude larger than those using the TL pulse. For the curve using the shaped pulse train, the intensity of the CE channel is stronger than that of the DI channel.

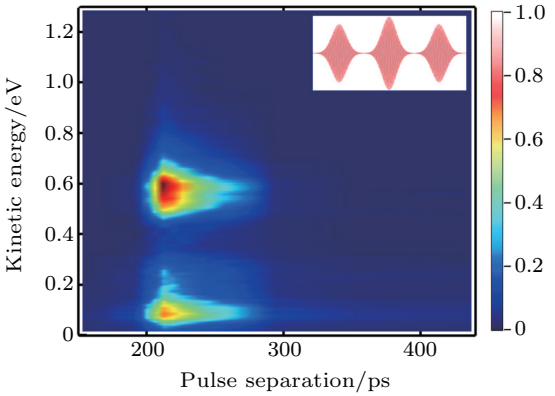


Fig. 3. The KER distributions upon the variation of the separation of shaped pulse train. The inset is the schematic diagram of the shaped pulse train.

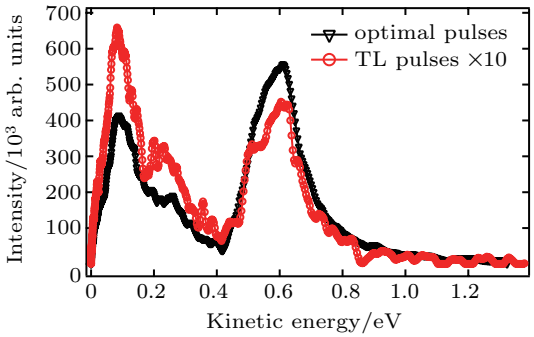


Fig. 4. The KER distributions using TL pulse (red) and optimal pulse train (black).

To investigate the control over different fragmentation channels of I^+ using shaped pulse train, we integrate the KER distribution respect to the corresponding peak to obtain the curves of the intensities of different channels with the pulse separation. Since the two peaks of the CE channels overlap, we integrate the two CE channels as one peak, and the same operation is performed for the two peaks of the DI channels.

Figure 5 shows the intensities of fragment ions I^+ from different channels as a function of the pulse separation (or the delay of pump–probe experiment). The intensities are normalized respect to that of the corresponding channel using TL pulse. Regardless of DI channels, CE channels, or all channels, the intensities (red curves) of fragment ion I^+ as a function of the pulse separation show the same patterns. When $T = 208$ fs, the intensities reach the maxima. The intensity of DI channel is 6 times higher than that of TL pulse, and those of CE channel and all channels are 7 times and 6.4 times, respectively. Compared with that of the DI channel, the intensity of the CE channel increases acutely, which will be discussed later in detail. In addition, the previous work of our research group[35] using shaped pulse train combined with TOFS performed the study on the DI processes of CH_3I molecule, wherein the same parametric values of the sinusoidal phase modulated function were chosen. The intensity of the fragment ion I^+ reached the maximum at $T = 200$ fs, which is almost consistent with the result of our present work ($T = 208$ fs). For the pump–probe experiment results (blue curves) in Fig. 5, we do not find significant modulation with the delay, and the intensities of fragment ions I^+ from all channels for pump–probe are lower than those for the shaped pulse near $T = 208$ fs. In addition, the energy of the shaped pulse train and pump–probe experiment is the same as that of the TL pulse.

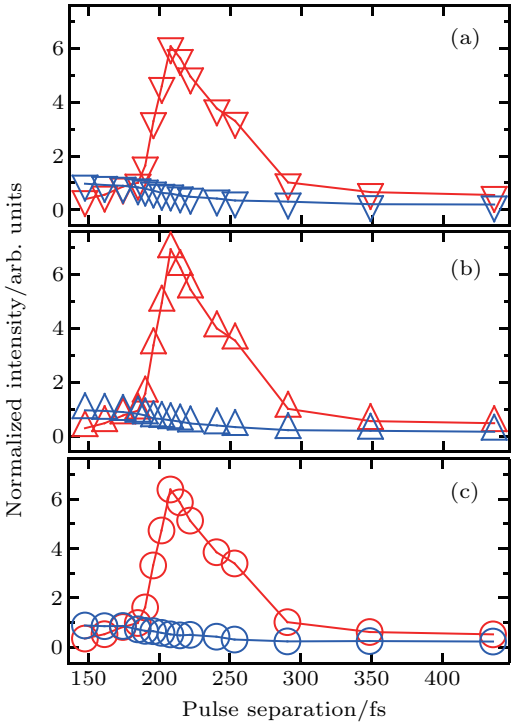


Fig. 5. The intensities of fragment ions I^+ from (a) DI, (b) CE, and (c) all channels as a function of the separation of the shaped pulse train. The intensities are normalized respect to that of the corresponding channel using TL pulse. The red (blue) curves are the results using the shaped pulse (pump–probe experiment).

Due to the short pulse duration, the dominant dissociation mechanism is DI. For the shaped pulse train, the equivalent duration is larger than that of the TL pulse. Moreover, because of the effect of multiple sub-pulses, the photodissociation of CH_3I in its A-band is likely to happen using the shaped pulse train. The dominant transition in A-band at the wavelength used in the present work is to the $^3Q_0$ state (parallel transition) by absorbing three 800 nm photons, which leads to direct C–I bond cleavage into a methyl radical and a spin–orbit excited iodine atom ($^2P_{1/2}$). Two weak transitions are accessible through dipole allowed transition: perpendicular transition to $^1Q_1$ and $^1Q_1 \leftarrow ^3Q_0$ via a curve crossing. Both transitions produce a methyl radical and a ground state iodine atom ($^2P_{3/2}$). The real time photodissociation dynamics of CH_3I from A-band have been studied using femtosecond pump–probe in combination with VMI, where the intensities of I atom, CH_3 radical and the ratio I/ CH_3 can be generally controlled.[25–27]

The control mechanism in the present study might be the modulation of A-band photodissociation, which ultimately leads to the modulation of intensity of the I^+ fragment ionized from the neutral iodine atom. However, the previous research results have confirmed that the dissociation time of all photodissociation channels from A-band is less than 150 fs.[36] For the optimal pulse train ($T = 208$ fs) in the present study, the photodissociation processes have already been completed before the arrival of the subsequent sub-pulses. Therefore, the control mechanism is not the modulation of the A-band photodissociation.

One possible way to rationalize the counterintuitive results is to consider the modulation of ionization processes of CH_3I under the irradiation of the shaped pulse train, where a qualitative control mechanism of the three pulses is proposed. This is mainly attributed to two reasons. One is that we did not see the modulation of iodide ion's intensity with the delay in the pump–probe experiment in Fig. 5. The intensity does not change significantly with the delay of pump–probe. The other is that the intensities of all fragment ions have increased significantly (the results will be presented and discussed in a follow-up paper). If the control is implemented via the modulation of the branching ratio of the dissociation channel, the intensities of all fragment ions will not increase, instead of the decrease of the fragment ion produced by the suppressed channel. We believe that the structure and phase of the shaped pulse rather than the effective duration is crucial to the modulation, which has been successfully proven in the frequency domain in our previous work.[33] This interesting and counterintuitive mechanism is attracting many researchers to carry out the study of shaped pulse coherent control. Because when the laser energy is the same, the intensity of the shaped pulse is lower than that of the TL pulse, but the yield of the shaped pulse is larger than that of the TL pulse. Figure 6 shows a

schematic illustration of the control mechanism. The ionization energy of CH_3I is about 9.54 eV, which indicates that the ionization from $CH_3I(X^1A_1)$ to $CH_3I^+(X^2E_{3/2,1/2})$ requires to absorb seven 800 nm photons via the multiphoton process. By absorbing photons from $X^2E_{3/2,1/2}$ to $B^2E_{3/2,1/2}$, CH_3I^+ dissociates into CH_3 and I^+. We call the former two sub-pulses ionizing pulses, the third sub-pulse dissociative pulse, and propose that the assembly of ionization processes is the coherent interference between the two independent wave packets excited by the two ionizing pulses in the time domain. The delay between two wave packets is determined by T. The difference of phase between the two wave packets is $\Phi_{\rm dif} = \Delta\omega T$,which is exactly the difference of phase between two adjacent sub-pulses. For this qualitative interference model, we assume that the ionization process is a transition from the ground state of the CH_3I molecule to the singlet excited state ($\omega_{\rm n}$). The ionization wave functions excited by the two ionizing pulses are simply written as

$$\psi_1 \propto A\,{\rm e}^{-{\rm i}\omega_{\rm n}t}, \tag{3}$$

$$\psi_2 \propto B\,{\rm e}^{-{\rm i}\omega_{\rm n}[(t+T)+\Phi_{\rm dif}]}, \tag{4}$$

where A and B are the constants associated with the transition probability. The interference of wave functions $\psi = \psi_1 + \psi_2$. The intensity of the total ionization processes measured in experiment is given by

$$I \propto A^2 + B^2 + AB\cos(\omega_{\rm n}T + \Phi_{\rm dif}). \tag{5}$$

From Eq. (5), we can deduce that the intensity of ionization oscillates and is modulated by T and $\Phi_{\rm dif}$ determined by the phase parameters of the shaped pulse train. Considering the interference of wave packets, only when the two wave packets are in phase (T and $\Phi_{\rm dif}$ are selected as few special values), the intensity of the total ionization processes will significantly enhance via constructive interference. However, the absence of modulation in the pump–probe experiment is because $\Phi_{\rm dif}$ is unlocked and unmodulated.

Therefore, for the three pulses control mechanism, the former two sub-pulses are the key to the modulation of yield of fragment ion I^+ for the DI channels. With the movement of the wave packet on the potential energy surface, the delay T determines the photon energy of the transition from $X^2E_{3/2,1/2}$ to dissociation state $B^2E_{3/2,1/2}$. After the unique delay of T, the third sub-pulse arrives and maximizes the fragmentation. The two processes of ionization interference and maximizing dissociation work together and lead to the modulation of the I^+ fragment yield. This is the reason that the peak intensities of KER distribution in Fig. 3 and the yield of I^+ in Fig. 5 do not oscillate with the pulse separation. In addition, we believe that the narrower scan range of pulse separation in our experiment might not show the whole oscillation period determined by $\omega_{\rm n}$. As the pulse separation gradually increases, the stronger vibrative decoherence effect of CH_3I (< 1 ps) will also significantly reduce the yield and dissipate the oscillation.

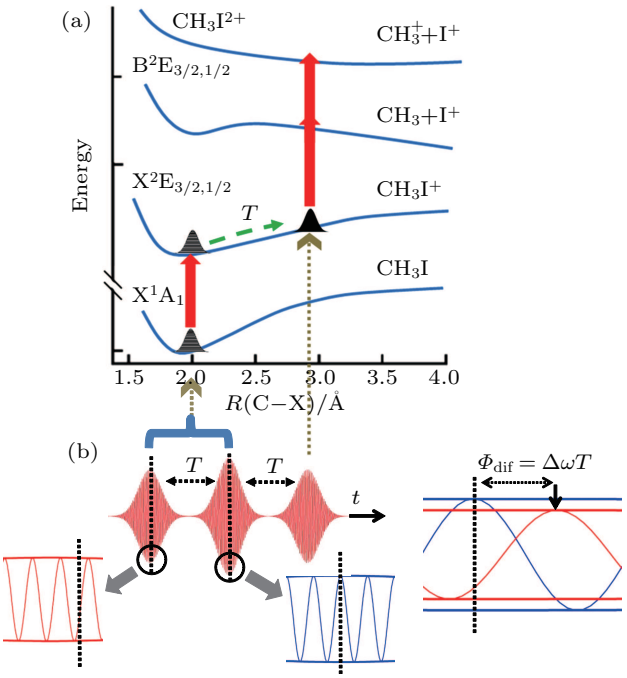


Fig. 6. Schematic diagram of the control mechanism for DI channel. (a) The assemble of ionization processes is the coherent interference between the two independent wave packets excited by the former two ionizing pulses in the time domain. After a delay of T, the third sub-pulse arrives and leads to the dissociation (DI and CE). (b) The temporal separation between adjacent sub-pulses is determined by the parameter T. The difference of relative phases between adjacent sub-pulses is determined by $\Phi_{\rm dif} = \Delta\omega T$.

Compared with the case under the TL pulse, the increase in intensity of CE channel is almost the same as that of DI channel using the shaped pulse train in Fig. 5. But it is difficult for two competitive dissociation mechanisms (DI and CE) to produce the same increase in yield. In addition, the intensities of all fragment ions have increased significantly. Therefore, we can infer that the modulation mainly occurs during the ionization processes, rather than during the dissociation processes. We believe that the same modulation mechanisms in DI and CE lead to the control on the yield of fragment ion I^+. As shown in Fig. 6, the former two sub-pulses cause the modulation of yield of fragment ion I^+ for the CE channels. After the unique delay of T, the third sub-pulse arrives and maximizes the fragmentation of the CE channels. In addition, most of studies show a purely repulsive character in the potential energy surface of doubly charged parent ions CH_3I^{2+}.[37,38] But $B^2E_{3/2,1/2}$ of the DI channel has a small potential well trapping a few particles, which leads to the increase in the yield of CE channels slightly higher than that of DI channels. Further research needs to be carried out in wave packet interference and decoherence effect in the time domain.

4. Conclusion

We perform a study of coherent control on fragmentation of CH_3I by shaped femtosecond pulse train. The dissociation channels of fragment ion I^+ using TL pulse are identified via the analysis of KER distribution. By changing the separation of the shaped pulse train, the modulation of the KER distribution of I^+ fragment is achieved. Moreover, it is the optimal pulse train (with $T = 208$ fs) that makes the intensities of dissociation channels simultaneously reach the maxima. Compared with the TL pulse, both yields of DI and CE channels significantly increase. A three-pulse control model is proposed to explain the counterintuitive experimental results. We believe that the modulation of ionization processes leads to the control over fragmentation of CH_3I using the shaped pulse train, The assembly of ionization processes is the coherent interference between the two independent wave packets excited by the two ionizing pulses in the time domain. When T and $\Phi_{\rm dif}$ are selected as few special values, the two wave packets are in phase, and the intensity of the total ionization processes significantly enhances via constructive interference. The third sub-pulse arrives and leads to the fragmentation. The present study is beneficial for us to understand the coherent control mechanism. The wave packet interference and decoherence effect during molecular dissociation processes will be further investigated in time domain using shaped pulse. In addition, the effect of alignment will also be studied by measuring the angular distributions of fragments.

References

[1] Ma R, Wu C, Xu N, Huang J, Yang H and Gong Q 2005 *Chem. Phys. Lett.* **415** 58
[2] Eppink A and Parker D H 1997 *Rev. Sci. Instrum.* **68** 3477
[3] Ashfold M N, Nahler N H and Orr-Ewing A J 2006 *Phys. Chem. Chem. Phys.* **8** 26
[4] Hertel I V and Radloff W 2006 *Rep. Prog. Phys.* **69** 1897
[5] Rijs A M, Janssen M H, Chrysostom E H and Hayden C C 2004 *Phys. Rev. Lett.* **92** 123002
[6] Gessner O, Lee A M and Shaffer J P 2006 *Science* **311** 219
[7] Witte T, Hornung T, Windhorn L, Proch D and Kompa K L 2003 *J. Chem. Phys.* **118** 2021
[8] Johnsson P, Mauritsson J, Remetter T, Huillier A L and Schafer K J 2007 *Phys. Rev. Lett.* **99** 233001
[9] Locht R, Dehareng D, Hottmann K, Jochims H W, Baumgartel H and Leyh B 2010 *J. Phys. B: At. Mol. Opt. Phys.* **43** 105101
[10] Poullain S M, Chicharro D V and Banares L 2017 *Phys. Chem. Chem. Phys.* **19** 7886
[11] Hu L L, Zhou Z M, Dong C W and Zhu Q H 2012 *J. Chem. Phys.* **137** 144302
[12] Wei Z R, Li J L, See S T and Loh Z H 2017 *J. Phys. Chem. Lett.* **8** 6067
[13] Wei Z R, Li J L, Yang M H and Loh Z H 2017 *Nat. Comm* **8** 735
[14] Yazawa H, Tanabe T, Okamoto T, Yamanaka M and Kannari F 2006 *J. Chem. Phys.* **124** 204314
[15] Breuning H G, Lauer A and Weitzel K M 2006 *J. Phys. Chem. A* **110** 20
[16] Singh K P, Kenfack A, Rost J M and Pfeifer T 2018 *Phys. Rev. A.* **97** 033406
[17] Graham P, Menkir G and Levis R J 2003 *Spectrochim. Acta Part. B* **58** 1097
[18] Sussman B J, Townsend D, Ivanov M Y and Stolow A 2006 *Science* **314** 278
[19] Corrales M E, GonzálezVázquez J, Balerdi G, Solá I R, Nalda R and Banres L 2014 *Nat. Chem.* **6** 785
[20] Thanopulos I and Shapiro M 2006 *J. Chem. Phys.* **125** 133314
[21] Katharine M and Rabitz H 2012 *Nat. Chem.* **4** 72
[22] Geremia J M, Zhu W S and Rabitz H 2000 *J. Chem. Phys.* **113** 10841
[23] Xie X, Doblhoff-Dier K and Kitzler M 2012 *Phys. Rev. Lett.* **109** 243001
[24] Strobel A, Lochschmidt A, Fischer I, Niedner-Schatteburg G and Bondybey V E 1993 *J. Chem. Phys.* **99** 733
[25] Trippel S, Stei M, Eichhorn C, Otto R, Hlavenka P, Weidemuller M and Wester R 2011 *J. Chem. Phys.* **134** 104306
[26] Gitzinger G, Corrales M E and Banares L 2010 *J. Chem. Phys.* **132** 234313
[27] Felix A, Burt M, Amini K and Rolles D 2018 *J. Chem. Phys.* **149** 204313
[28] Wei Z R, Tian L, Li J L and Loh Z H 2018 *J. Phys. Chem. Lett.* **9** 5742
[29] Zhou C, Tong Q N, Zhang C C and Hu Z 2015 *Chin. Phys. B* **24** 043303
[30] Dela Cruz J M, Pastirk I, Lozovoy V V, Walowicz K A and Dantus M 2004 *J. Phys. Chem. A* **108** 53
[31] Lozovoy V V, Pastirk I and Dantus M 2004 *Opt. Lett.* **29** 775
[32] Liu H, Yang Z, Gao Z and Tang Z 2007 *J. Chem. Phys.* **126** 044316
[33] Wang Y, Zhang S, Wei Z and Zhang B 2008 *J. Phys. Chem. A* **112** 3846
[34] Tong Q N, Lian Z Z, Qi H X, Chen Z and Hu zhan 2019 *Chin. Phys. B* **28** 33201
[35] Song Y D, Chen Zhou, Sun C K and Hu Z 2013 *Chin. Phys. B* **22** 013302
[36] Nalda R, Izquierdo J G, Dura J and Banares L 2007 *J. Chem. Phys.* **126** 021101
[37] Corrales M E, GonzálezV ázquez J and Banres L 2012 *J. Phys. Chem. A* **116** 2669
[38] Luo S Z, Hu W H, Yu J Q, Li X K and Ding D J 2017 *J. Phys. Chem. A* **121** 6547